DOI: 10.1002/cssc.201100284

# Mesoporous Nitrogen-Rich Carbon Materials as Catalysts for the Oxygen Reduction Reaction in Alkaline Solution

Tharamani C. Nagaiah,*[a] Ankur Bordoloi,[b] Miguel D. Sánchez,[b, c] Martin Muhler,*[b] and Wolfgang Schuhmann[a]

The electrochemical reduction of molecular oxygen is highly relevant for devices such as metal–air batteries, fuel cells, and air-breathing cathodes in industrial electrocatalytic processes. One of the most important applications of the oxygen reduction reaction (ORR) is the cathodic reaction in fuel cells. Poor kinetics for the ORR in fuel cell cathodes and the high costs of platinum-based catalysts are the major factors retarding the implementation of low-temperature fuel cells. In order to be competitive in mainstream commercial markets, fuel cells have to become more cost-effective and highly durable, and many research efforts have therefore been devoted to the search for less-expensive and highly stable cathode catalysts.

Carbon materials have been suggested as promising non-precious metal catalysts for the ORR.[1] Although the detailed mechanism of the ORR at carbon-based materials remains unclear, the specific properties of the exposed carbon surfaces were found to have a substantial influence on the ORR kinetics. Hence, the modification of carbon electrode surfaces for enhancing the electrocatalytic activity has become a highly interesting research topic. For example, nitrogen-functionalized carbon nanotubes,[2,3] mesoporous carbon treated with ammonia,[4] and nitrogen-doped graphitic carbon[5] have been applied as active catalysts for the ORR or can be used as catalyst support. The presence of either pyridinic or pyrrolic/pyridinic[6] and/or quaternary[7] nitrogen species is supposed to be responsible for the enhanced ORR activity. In many of these materials these functional groups are generated via chemical pretreatment with reactive species such as $HNO_3$, $NH_3$, or HCN.[8] More importantly, these processes suffer from several disadvantages, such as requiring multistep procedures to introduce the nitrogen functional groups, leading to a poor control over the chemical homogeneity and reproducibility, long preparation times, and sometimes deterioration of the structure of the materials. Consequently, the development of metal-free highly active catalysts with similar properties based on facile, versatile, inexpensive, and reproducible syntheses is of high importance.

Mesoporous carbon nitride is a material with unique structural properties, such as a high specific surface area and pore volume, tunable pore sizes, relatively high inertness, and resistance to high pressure and temperatures.[9] Particularly, it has a graphite-like structure with pyridine-like nitrogen atoms. Here, we explored related and previously synthesized, but structurally less-well-defined mesoporous nitrogen-rich carbon (MNC) materials[9d,e] as metal-free catalysts for the ORR. The fabrication procedure of such materials can be easily scaled up for mass production, and there is no need for a post-synthesis introduction of functional nitrogen groups to these MNC materials, as in the case of nitrogen-modified carbon nanotubes or other previously reported materials.[2–4] The MNC materials exhibit excellent catalytic ORR activity in alkaline medium with lower overpotential and better long-term stability than a commercial Pt/C catalyst and similar nitrogen-doped carbon materials. To the best of our knowledge, MNC materials have not been previously investigated as electrocatalysts for the ORR.

The MNC materials were synthesized by pyrolyzing polymerized ethylenediamine nanocasted into a SBA-15 hard template based on a procedure from Ref. [9d] at temperatures of 400 (MNC-400), 600 (MNC-600), and 800 °C (MNC-800), followed by the dissolution of the silica framework. The morphology and mesoporosity of the MNC catalysts were not destroyed with increasing pyrolysis temperature, as confirmed by scanning electron microscopy (SEM, Figure S1, Supporting Information). High-resolution transmission electron microscopy (HRTEM) images show the well-ordered structure of MNC-800, as evident by the regular linear array of mesopores (Figure 1b) and X-ray diffraction results (XRD; Figure 2). The wide-angle diffraction pattern of the MNC materials (Figure 2, inset) exhibits a broad peak around 26°, originating from the (002) plane of graphitic carbon. A broad peak around 43° appears in the spectra of the MNC-600 and the MNC-800 catalysts, due to the (100) reflection of graphitic carbon. Small-angle XRD measurements (Figure 2) reveal a peak in the range between 0.5 and 6°, which can be indexed to the (100) reflection of the hexagonal *p6mm* space group. A very small peak was additionally observed in both MNC-600 and MNC-800, which is supposed to be due to the related (110) plane. These observations are in good agreement with the XRD pattern of the pure hexagonally ordered SBA-15 material (Figure 2) and previously reported results,[10] indicating that the MNC materials have a well-ordered

[a] *Dr. T. C. Nagaiah, Prof. Dr. W. Schuhmann*
*Analytische Chemie-Elektroanalytik & Sensorik*
*and Center for Electrochemical Sciences-CES*
*Ruhr-University Bochum*
*44780 Bochum (Germany)*
*Fax: (+49) 234-32-14683*
*E-mail: tharamani.chikka-nagaiah@rub.de*

[b] *Dr. A. Bordoloi, Dr. M. D. Sánchez, Prof. Dr. M. Muhler*
*Laboratory of Industrial Chemistry*
*Ruhr-University Bochum*
*44780 Bochum (Germany)*
*Fax: (+49) 234-32-14115*
*E-mail: muhler@techem.rub.de*

[c] *Dr. M. D. Sánchez*
*Instituto de Fisica del Sur and Departmento de Fisica*
*Universidad Nacional del Sur-CONICET*
*8000 Bahia Blance (Argentina)*

Supporting Information for this article is available on the WWW under http://dx.doi.org/10.1002/cssc.201100284.

  

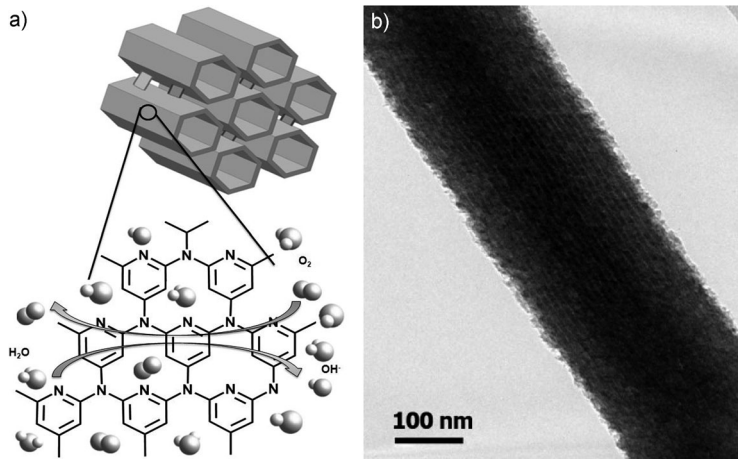


**Figure 1.** a) Schematic ideal structure of mesoporous carbon nitride, adapted from Ref. [9d]. b) HRTEM image of the MNC catalyst, pyrolyzed at 800 °C.

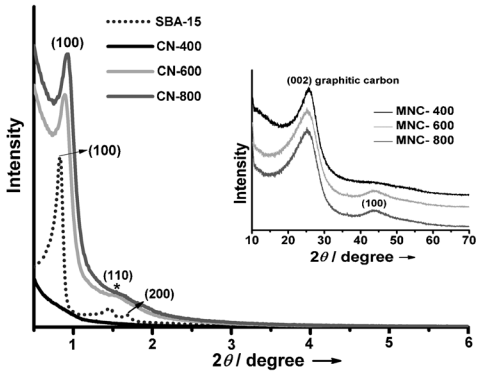


**Figure 2.** Small- and wide-angle (inset) X-ray diffraction patterns of the MNC catalysts, pyrolyzed at different temperatures.

two-dimensional mesoporous structure with a hexagonal porous network.

The $N_2$ physisorption isotherms of MNC-600 and MNC-800 exhibit type IV shapes (Figure S2, Supporting Information), with a H1 hysteresis loop with capillary condensation at a relative pressure $p/p_o \approx 0.4$–$0.8$, characteristic for ordered mesoporous materials. MNC-600 has a maximum Barrett–Joyner–Halenda (BJH) pore diameter of 3.8 nm and a specific Brunauer–Emmett–Teller (BET) surface area of 473 $m^2 g^{-1}$. Interestingly, MNC-800 shows a higher surface area of 517 $m^2 g^{-1}$ with a similar pore diameter of 3.8 nm. The pore volume is found to be higher in case of MNC-800 (0.6 $mL g^{-1}$) compared to MNC-600 (0.4 $mL g^{-1}$), which could be due to the formation of a higher number of micropores at the higher pyrolysis temperature.

To investigate the electrocatalytic activity of the MNC catalysts and to compare the effect of the pyrolysis temperature on the ORR, cyclic voltammetry (CV) and rotating disc electrode (RDE) measurements were carried out in a potential window from 0.4 to −0.6 V at a scan rate of 5 $mV s^{-1}$ vs. a double-junction Ag/AgCl/3 M KCl reference electrode. A first set of experiments was performed in $O_2$-free 1 M NaOH solution obtained by purging with Ar for 30 min before each measurement. In the absence of $O_2$, the voltammograms did not show any characteristic oxidation/reduction peaks. However, the capacitive current increased substantially as compared to a bare glassy carbon electrode due to the increase in surface area. Significant changes can be observed in the CVs after saturation of the 1 M NaOH solution with $O_2$, achieved by purging with $O_2$ for 20 min before each measurement and above the electrolyte solution during the measurements. The voltammograms show the increase in the current density ($j_k$) for the ORR (Figure S3; Supporting Information), confirming that the prepared MNC materials are electrocatalytically active for the ORR. A remarkable increase in the catalytic activity with increasing pyrolysis temperature was observed with respect to both the reduction current and the shift in the onset potential for the ORR.

RDE measurements were performed in order to further quantify the ORR activities and compare them with that of a commercial Pt/C (20% Pt) catalyst. Figure 3a shows the ORR polarization curves in the presence of $O_2$. The significant changes in $j_k$ and the shift of the ORR onset potential for the MNC samples pyrolyzed at different temperatures are clearly visible. Further, with increase in pyrolysis tempera-

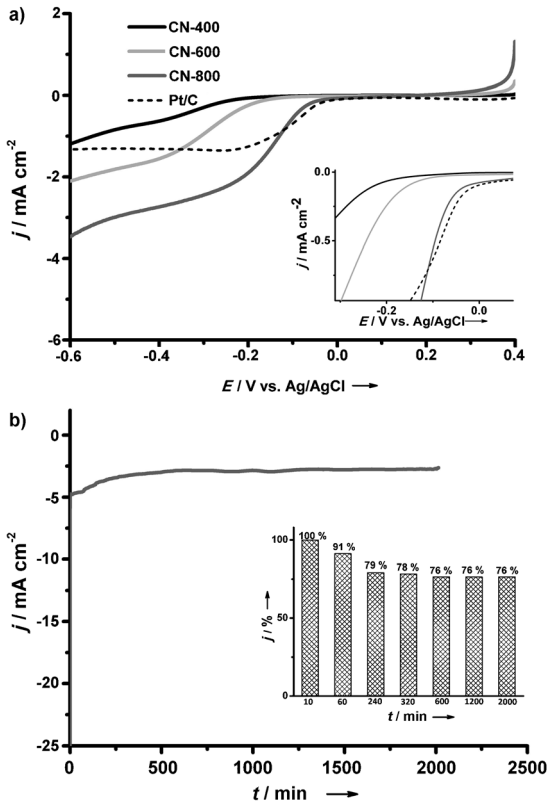


**Figure 3.** a) Polarization curves of MNC catalysts pyrolyzed at different temperatures in $O_2$-saturated 1 M NaOH with a rotation rate of 900 rpm at a scan rate of 5 $mV s^{-1}$, CE: Pt grid, RE: Ag/AgCl/3 M KCl (inset: magnification of the potential region of the ORR onset). b) Chronoamperometric measurements of MNC-800 at −0.3 V (inset: bar diagram showing the relative decrease of the current density with time).

  

ture, the onset potentials shifted towards anodic potentials from −0.19 V (MNC-400) to −0.13 V (MNC-600) and +0.03 V for MNC-800 at a current density of $j_K = -0.06$ mA cm$^{-2}$. Interestingly, $j_k$ also increases from −1.18 mA cm$^{-2}$ (MNC-400) to −3.5 mA cm$^{-2}$ (MNC-800) at a potential of −0.6 V with increasing pyrolysis temperature, which is supposed to be due to the not completely formed mesoporous structure of MNC-400 (Figure S1 A, Supporting Information). Surprisingly, the commercial Pt/C catalyst has an onset potential of 0.02 V, but shows a significant lower ORR activity evident from its lower $j_k$ of −1.3 mA cm$^{-2}$. Evidently, this observation is either due to an active site limitation of the current density for the Pt/C modified electrode in alkaline solution or to a lower average number of electrons transferred per $O_2$ molecule. The increase of the current density at lower potentials as well as the less steep current decrease in the kinetic region of the polarization curve of the MNC materials is due to the mesoporosity of the material, which is increasing the probability of re-adsorption of potentially primarily formed $H_2O_2$ and consecutive electron-transfer steps.

Despite the fact that the analysis of the kinetic parameters for the ORR using Koutecky–Levich (KL) plots (Figure S5, Supporting Information) is only considered to be a rough estimation for mesoporous materials, the number of electrons transferred during the oxygen reduction was estimated to be 3.8 for MNC-800.

The XPS C 1s spectra of the MNC-400, MNC-600, and MNC-800 samples are shown in Figure 4 a. The spectra were deconvoluted into seven components. The two main peaks at 284.5 and 285.3 eV were assigned to sp$^2$-hybridized graphite-like carbon (C–C sp$^2$) and sp$^3$-hybridized diamond-like carbon (C–C sp$^3$), respectively, overlapping with sp$^2$ carbon bound to

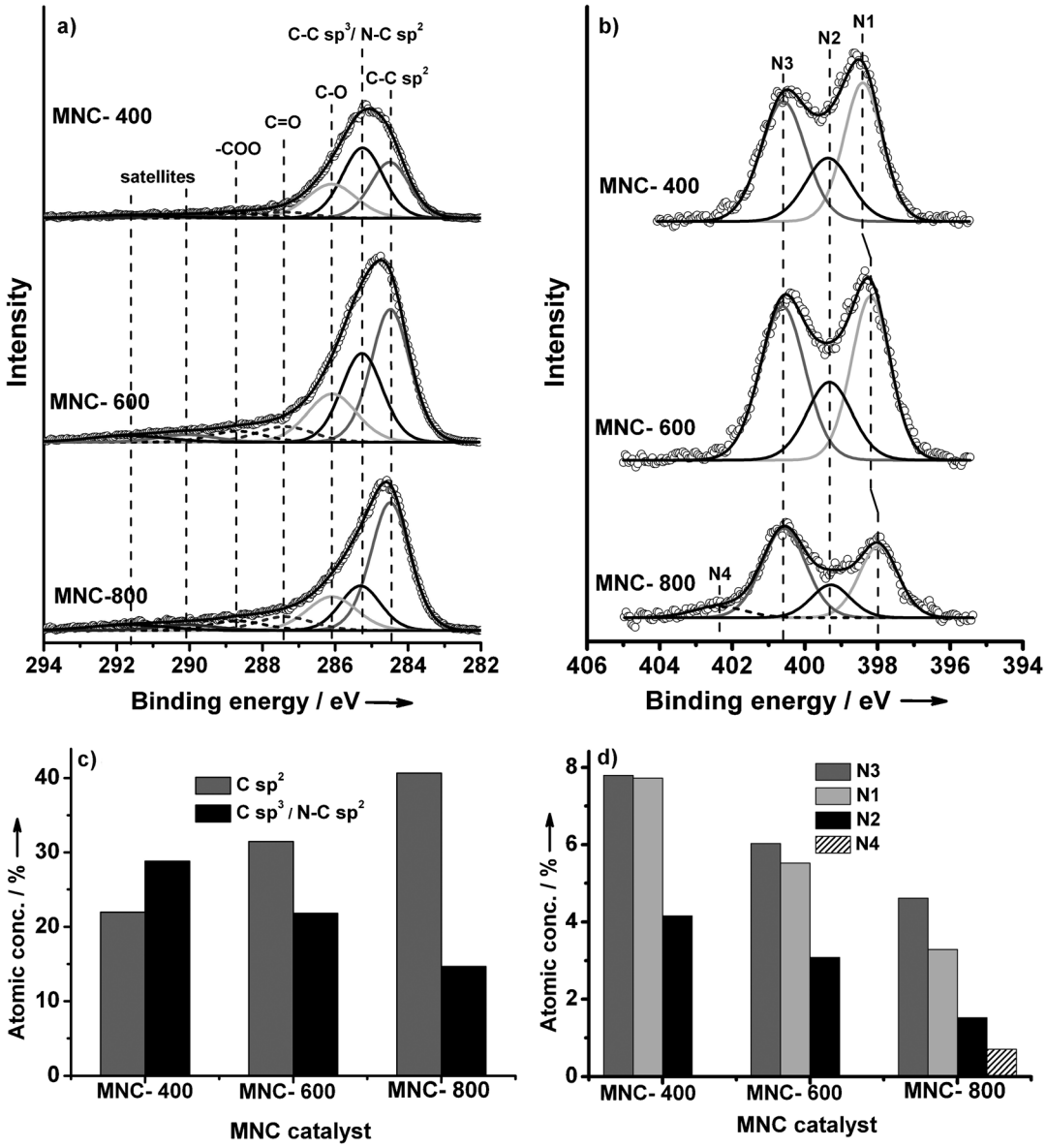


**Figure 4.** Deconvoluted XPS spectra of a) C 1s, and b) N 1s, and c, d) bar diagrams representing the variation of the atomic surface concentration of different carbon species and nitrogen functional groups, respectively, for the different MNC catalysts.

  

nitrogen (N–C $sp^2$). The peaks centered at 286.1, 287.4, and 288.7 eV were attributed to surface oxygen groups (designated as C–O, C=O and –COO, respectively), and the additional features at 290.1 and 291.7 eV are satellites of $sp^2$ graphite-like carbon in good agreement with literature.[11–13]

The N 1s region (Figure 4b) exhibits three main contributions: the peak at the lowest binding energy (N1) shifting from 398.4 eV for MNC-400 to 398.0 eV for MNC-800 originates from pyridinic nitrogen. The peak at 399.3 eV (N2) is assigned to pyrrolic nitrogen, and the peak at 400.6 eV (N3) indicates the presence of quaternary nitrogen.[11–13] The minor N 1s peak at 402.4 eV (N4) originates from the N-oxide of pyridinic nitrogen.[11,12] These findings further support the initial assumption that the material is structurally much less ideal than carbon nitride, providing a variety of different potential adsorption sites for $O_2$ and the reaction intermediates.

The surface atomic concentration ratios were derived from the XPS spectra as shown in Figure 4c and 4d. With increasing pyrolysis temperature, a noticeable decrease of the $sp^3$ carbon concentration associated with an increase in the $sp^2$ carbon concentration was observed (Figure 4c). This observation is in good agreement with the XRD results, demonstrating a well-ordered graphite-like surface structure for MNC-600 and MNC-800. The signal at 285.3 eV (Figure 4A) is mainly due to carbon atoms bound to nitrogen atoms (N–C $sp^2$). The surface concentrations of the different nitrogen species are shown in Figure 4d, in which an appreciable decrease of all nitrogen surface species can be observed. In addition, the MNC materials were characterized by $^{13}C$ NMR spectroscopy in order to identify the nature and environment of the carbon and nitrogen atoms. As seen from Figure S6 (Supporting Information), the MAS spectra exhibit one broad asymmetric peak: the larger sharp peak at 123.95 ppm can be attributed to $sp^2$ carbon atoms directly bound to carbon, whereas the broad shoulder at 135–160 ppm can be assigned to $sp^2$ carbon atoms bound to nitrogen.[9d]

The durability of the catalysts and the long-term stability of the electrocatalytic activity for the ORR are of major concern in the development of fuel cells. In order to evaluate the stability of the electrocatalytic properties of MNC-800, chronoamperometric measurements in $O_2$-saturated 1 M NaOH were performed while simultaneously rotating the electrode. A constant potential of −0.3 V and a rotation rate of 900 rpm were applied, and the current density was plotted as a function of time (Figure 3b). After an initial decay of the oxygen reduction current density, a constant value is reached after about 60 min at about 80% of the initial activity, demonstrating a good long-term stability of its electrocatalytic properties on the timescale of hours in the alkaline medium.

The following properties of MNC-800 are considered to be relevant for its observed enhanced ORR electrocatalytic activity: The surface area and pore volume increase with increasing pyrolysis temperature as derived from the $N_2$ physisorption isotherm (Figure S2, Table S1, Supporting Information), which are assumed to lead to improved mass transfer for MNC-800 as compared with MNC-600. The presence of the nitrogen functional groups and the graphitic nature of the catalysts are both considered essential for high ORR activity. Our results imply that also the higher degree of graphitization (Figure 4c) contributes to the higher activity of MNC-800.[5,14] This is further supported by the oxidation of the MNC materials studied by thermogravimetric analysis in the presence of air. As can be seen in Figure S7 (Supporting Information), the oxidation of MNC-400 started below 400 °C, which is due to the presence of more amorphous carbon in the catalyst. However, for MNC-800 the highest oxidation onset temperature was found indicating a higher degree of graphitization in agreement with the XPS results.

In summary, mesoporous nitrogen-rich carbon materials synthesized by pyrolysis at 800 °C exhibit an interestingly high electrocatalytic activity in the ORR, and they may be further exploited as potentially efficient and inexpensive metal-free ORR catalysts with good long-term stability in alkaline solution.

## Experimental Section

Experimental details are provided in the Supporting Information.

## *Acknowledgements*

*T.C.N. and A.B. thank the Alexander-von-Humboldt Foundation for postdoctoral fellowships. The authors are grateful to Dr. Vasanthakumar G. Ramu for useful discussions, and to the EU and the state of North-Rhine-Westphalia for financial support in the framework of the Hightech.NRW project CES.*

**Keywords:** electrocatalytic activity · mesoporous nitrogen-rich carbon materials · oxygen reduction reaction · RDE · XPS

[1] a) P. J. Britto, K. S. Santhanam, A. Rubio, J. A. Alonso, P. M. Ajayan, *Adv. Mater.* **1999**, *11*, 154–157; b) G. Che, B. B. Lakshmi, C. R. Martin, E. R. Fisher, *Langmuir* **1999**, *15*, 750–758; c) W. Z. Li, C. H. Liang, J. S. Qiu, W. J. Zhou, H. M. Han, Z. B. Wei, G. Q. Sun, Q. Xin, *Carbon* **2002**, *40*, 791–794.

[2] T. C. Nagaiah, S. Kundu, M. Bron, M. Muhler, W. Schuhmann, *Electrochem. Commun.* **2010**, *12*, 338–341.

[3] K. P. Gong, F. Du, Z. H. Xia, M. Durstock, L. M. Dai, *Science* **2009**, *323*, 760–764.

[4] a) X. Q. Wang, J. S. Lee, Q. Zhu, J. Liu, Y. Wang, S. Dai, *Chem. Mater.* **2010**, *22*, 2178–2180; b) W. Yang, T.-P. Fellinger, M. Antonietti, *J. Am. Chem. Soc.* **2011**, *133*, 206–209.

[5] R. Liu, D. Wu, X. Feng, K. Müllen, *Angew. Chem.* **2010**, *122*, 2619–2623; *Angew. Chem. Int. Ed.* **2010**, *49*, 2565–2569.

[6] a) J. I. Ozaki, S. I. Tanifuji, N. Kimura, A. Furuichi, A. Oya, *Carbon* **2006**, *44*, 1324–1326; b) S. Kundu, T. C. Nagaiah, W. Xia, Y. M. Wang, S. van Dommele, J. H. Bitter, M. Santa, G. Grundmeier, M. Bron, W. Schuhmann, M. Muhler, *J. Phys. Chem. C* **2009**, *113*, 14302–14310.

[7] H. Niwa, K. Horiba, Y. Harada, M. Oshima, T. Ikeda, K. Terakura, J. Ozaki, S. Miyata, *J. Power Sources* **2009**, *187*, 93–97.

[8] a) J. Mrha, *Collect. Czech. Chem. C* **1967**, *32*, 708–719; b) P. Vinke, M. van der Eijk, M. Verbree, A. F. Voskamp, H. van Bekkum, *Carbon* **1994**, *32*, 675–686; c) J. Lahaye, G. Nanse, A. Bagreev, V. Strelko, *Carbon* **1999**, *37*, 585–590.

[9] a) X. F. Chen, Y. S. Jun, K. Takanabe, K. Maeda, K. Domen, X. Z. Fu, M. Antonietti, X. C. Wang, *Chem. Mater.* **2009**, *21*, 4093–4095; b) B. V. Lotsch, W. Schnick, *Chem. Mater.* **2006**, *18*, 1891–1900; c) A. H. Lu, B. Spliethoff, F. Schüth, *Chem. Mater.* **2008**, *20*, 5314–5319; d) A. Vinu, *Adv. Funct. Mater.* **2008**, *18*, 816–827; e) A Vinu, P. Srinivasu, D. P. Sawant, T. Mori, K.

  

Ariga, J.-S. Chang, S.-H. Jhung, V. V. Balasubramanian, Y. K. Hwang, *Chem. Mater.* **2007**, *19*, 4367 – 4372.
[10] D. Zhao, Q. S. Huo, J. L. Feng, B. F. Chmelka, G. D. Stucky, *J. Am. Chem. Soc.* **1998**, *120*, 6024 – 6036.
[11] S. Kundu, W. Xia, W. Busser, M. Becker, D. A. Schmidt, M. Havenith, M. Muhler, *Phys. Chem. Chem. Phys.* **2010**, *12*, 4351 – 4359.
[12] R. Arrigo, M. Hävecker, R. Schlögl, D. S. Su, *Chem. Commun.* **2008**, 4891 – 4893.
[13] V. N. Khabashesku, J. L. Zimmerman, J. L. Margrave, *Chem. Mater.* **2000**, *12*, 3264 – 3270.
[14] T. Ikeda, M. Boero, S. F. Huang, K. Terakura, M. Oshima, J. Ozaki, *J. Phys. Chem. C* **2008**, *112*, 14706 – 14709.

Received: June 7, 2011
Revised: October 11, 2011
Published online on March 16, 2012

  